

Article

Hybrid State of Charge Estimation of Lithium-Ion Battery Using the Coulomb Counting Method and an Adaptive Unscented Kalman Filter

Hend M. Fahmy¹, Rania A. Swief¹, Hany M. Hasanien^{1,2,*}, Mohammed Alharbi³, José Luis Maldonado⁴ and Francisco Jurado⁴

¹ Electrical Power and Machines Department, Faculty of Engineering, Ain Shams University, Cairo 11517, Egypt; hendmustafa26@gmail.com (H.M.F.); rania.swief@gmail.com (R.A.S.)

² Faculty of Engineering and Technology, Future University in Egypt, Cairo 11835, Egypt

³ Electrical Engineering Department, College of Engineering, King Saud University, Riyadh 11421, Saudi Arabia; mohalharbi@ksu.edu.sa

⁴ Department of Electrical Engineering, Superior Polytechnic School of Linares, University of Jaén, 23700 Linares, Spain; jlmo0003@red.ujaen.es (J.L.M.); fjurado@ujaen.es (F.J.)

* Correspondence: hanyhasanien@ieee.org

Abstract: This paper establishes an accurate and reliable study for estimating the lithium-ion battery's State of Charge (SoC). An accurate state space model is used to determine the parameters of the battery's nonlinear model. African Vultures Optimizers (AVOA) are used to solve the issue of identifying the battery parameters to accurately estimate SoC. A hybrid approach consists of the Coulomb Counting Method (CCM) with an Adaptive Unscented Kalman Filter (AUKF) to estimate the SoC of the battery. At different temperatures, four approaches are applied to the battery, varying between including load and battery fading or not. Numerical simulations are applied to a 2.6 Ahr Panasonic Li-ion battery to demonstrate the hybrid method's effectiveness for the State of Charge estimate. In comparison to existing hybrid approaches, the suggested method is very accurate. Compared to other strategies, the proposed hybrid method achieves the least error of different methods.

Keywords: Li-ion batteries; battery management system (BMS); state of charge (SoC); battery model; parameter identification; Kalman filters; coulomb counting method (CCM)



Citation: Fahmy, H.M.; Swief, R.A.; Hasanien, H.M.; Alharbi, M.; Maldonado, J.L.; Jurado, F. Hybrid State of Charge Estimation of Lithium-Ion Battery Using the Coulomb Counting Method and an Adaptive Unscented Kalman Filter. *Energies* **2023**, *16*, 5558. <https://doi.org/10.3390/en16145558>

Academic Editor: Fangming Jiang

Received: 16 June 2023

Revised: 5 July 2023

Accepted: 12 July 2023

Published: 22 July 2023



Copyright: © 2023 by the authors. Licensee MDPI, Basel, Switzerland. This article is an open access article distributed under the terms and conditions of the Creative Commons Attribution (CC BY) license (<https://creativecommons.org/licenses/by/4.0/>).

1. Introduction

Energy storage systems (ESS) are becoming essential in modern power networks to the growing use of renewable energy sources, characterized by uncertainty and fluctuation [1]. In addition to their fundamental role in storage and retrieval, energy storage components are crucial to providing auxiliary services to the hosting system. In numerous applications, including those involving portable electronics, electric cars, satellite components, and power systems, batteries of various kinds play a crucial role [2]. Compared to other common battery types, Li-ion batteries have a high energy density, a low self-discharge rate, and a long service life, making them a flexible and promising technology [3]. However, overcharging or undercharging Li-ion batteries can permanently harm the battery cells, reducing lifetime and degrading performance. Therefore, one of the critical purposes of BMS is to accurately estimate SoC to lower safety risks and extend the battery's health [4]. To determine the battery's SoC in real-time, the Battery Management System (BMS) observes battery measurements such as voltage, current, temperature, and other variables. Then, to prohibit overcharging and over-discharging the battery, preserve the battery's health, and extend its service life, it designs a reasonable approach to the charging and discharging phenomena of the Li-ion battery [5].

1.1. Problem under Study

Measuring the SoC of a Li-ion battery has proven to be a significant obstacle to correctly estimating it. Due to the intricate electrochemical processes taking place inside a Li-ion battery [6], SoC is not directly measurable due to the nonlinear connection between the SoC and OCV of the battery. It must be measured using voltage, current, and temperature measurements; hence why the precise calculation of SoC for battery simulation is a current research topic [7]. Accurate SoC estimation is a primary task in BMS by helping to improve the system implementation and precision and lengthening the service life of the battery [8]. It can also prevent unexpected system outages, keep the Li-ion battery from being overcharged or under-charged, which might permanently harm the battery's internal structure, and it enables the development of logical control schemes for energy conservation [9].

Before estimating SoC, precisely modeling the Li-ion battery characteristics using an Equivalent Circuit Model (ECM) is conducted, which include the battery's series resistance—the transient branch, which consists of polarization resistance and capacitance, and the OCV of the battery at different SoC values—different temperatures, and different loading and battery fading conditions, then estimating SoC by predicting the value of the state of charge, and then correcting the value of state by using the measurements of voltage, current, and temperature [10]. This will result in a precise state of charge assessment and battery modeling, which aids in the process of researching the Li-ion battery's dynamic reaction.

1.2. Literature Review

SoC is indicated as the battery's charge level, which reflects how much charge is still available in the battery cell compared to its capacity [11]. The SoC value ranges from 0 to 100% and is a relative number given as a percentage [12]. A Li-ion battery's SoC may be calculated using various techniques, such as direct measurement, bookkeeping, model-based, and hybrid methods [13].

Each strategy has unique traits and circumstances in which it works best. The Direct Measurement method measures SoC indirectly by using physical battery properties such as OCV and impedance, the most used being the Open-Circuit Voltage method [14], which measures SoC through an indirect relation between the SoC and OCV relation curve. However, to measure OCV correctly, it must be left unattended for a lengthy time, which is impractical in actual operations. To obtain an accurate SoC value, Wu et al. [15] provided the OCV calculation equation and estimated the OCV with voltage at a specific time after the battery stopped discharging. However, this method is still impractical because the battery must still stop discharging to measure SoC accurately. The impedance measurement method has the same issue, and the battery life cycle lengthens the impedance changes. Also, it is very responsive to temperature changes; SoC measurements are very challenging when the battery temperature fluctuates significantly [16]. The internal impedance impact when the battery drains cause a terminal voltage decrease, which is the basis for the terminal voltage technique. Since each of these is precisely proportional to SoC, it is presumed that the EMF of the Li-ion battery is direct to the terminal voltage. The predicted inaccuracy of the terminal voltage approach is significant because of the abrupt decrease in terminal voltage after the discharging phase, even though this method has been used at various drainage currents and temperatures [17].

Battery discharge information is used as input in the bookkeeping estimate technique. It enables several internal battery impacts in SoC estimation, such as self-discharge [18]. The most used method is the CCM which is also called the (Ah) Integration Method [19]. This technique works by multiplying the overall capacity by the current flowing and draining from the Li-ion battery, and is simple and cheap, but its major disadvantages are that any error in the current measurement will accumulate, making the measurements converge from the actual value.

Model-based estimation approach establishes a Li-ion battery model and combines several state-of-charge estimation algorithms to estimate SoC. One of the most essential estimation methods is that of adjustable systems [20]. These are self-designing systems, also known as observers, that can be spontaneously modified to accommodate any system changes. One of the most commonly used adjustable systems in batteries is the EKF [21], which uses the Taylor expansion approach to extend the traditional Kalman Filter for nonlinear models to estimate first and second-order derivatives. It estimates states of discrete time by taking two points (mean and approximate). This method yields good results, but due to only using the first term of expansion, the solutions in highly nonlinear systems are not accurate; therefore, another filter named the UKF is used [22]. It is a member of the more significant class of filters known as Sigma Point Kalman Filters, which employ statistical linearization, and estimates states of discrete time by using a collection of points called sigma points and approximate points. It then uses nonlinear transformations on the set of sigma points that are chosen deterministically, with very accurate solutions in highly nonlinear systems. For the standard EKF and UKF, they assume fixed uncertainties in error parameters, and these uncertainties propagate through the filter, which limits its effectiveness. Therefore, the Adaptive Kalman Filter (AKF) is used [23,24]. It adapts to any changes in data or the uncertainties of the error by defining some parameters of the model that are unknown, which makes it more accurate. It uses two independent models to estimate the state of a dynamic system: an observation model that establishes a link between measurements and the state vector, and a dynamic model that defines the behavior of the state vector. Adaptive systems provide a valuable option for SoC estimation since Li-ion batteries have nonlinear SoC relationships and are influenced by several chemical effects.

Hybrid methods [25] are models between different estimation techniques. Since the amount of information that can be gained from a single estimation approach is restricted, hybrid models aim to combine the benefits of each method and achieve an optimal estimation. A hybrid approach between several estimate algorithms may use the most significant benefits of various SoC estimation approaches, merge single model inputs, and maximize the available information, increasing estimation accuracy. There are several types of hybrid methods. The first is a combination of the Coulomb Counting (CCM) and EMF method, an innovative SoC estimating technique that has been devised and applied in an actual SoC estimation system. It combines the use of direct measurements, battery EMF measurements during the equilibrium stage, and bookkeeping estimations using the CCM approach during the discharge condition [26]. The second method is a combination between CCM and the Kalman Filter. Wang et al. [27] proposed an SoC estimation method where the Kalman Filter corrects the initial value used for the CCM, and then the CCM estimates SoC for the long working time. The third method is a combination between the Per-Unit System and Extended Kalman Filter (EKF). Kim et al. [28] explained the application of this combination to characterize the battery model parameters for very precise SoC estimation, using the battery parameters that are impacted by the aging effect, according to the PU system. In the equivalent circuit model, the terminal voltage of the battery and current, as well as the absolute parameter values, are modified into dimensionless magnitudes concerning a set of base magnitudes. The modified magnitudes are then applied to dynamic and observation models in the EKF method.

These approaches have yielded good outcomes but are short in accuracy and consistency. This study recommends the usage of the hybrid method by combining the CCM and various Kalman Filter approaches to minimize the error of the simulated and experimented SoC by using the Integral Square Error (ISE) method. First, defining the battery model parameters ensures optimal battery performance and longevity since any SoC estimate technique requires an accurate battery model. The battery parameters are established using (AVOA) [29] under various loading, fading, and temperature situations. The OCVs under various SoCs, R_o , and R_{tr} and C_{tr} are the design parameters that have been observed, then the SoC is estimated by using the combination of the Coulomb Counting Method (CCM)

and an Adaptive Unscented Kalman Filter (AUKF). AVOA validates the least error between various optimization algorithms, and the hybrid method validates the Li-ion batteries model's primary purpose with the least error. These skills provide the most accurate battery model with the best SoC estimation technique. Despite its advantages, it has not yet been employed to solve technical problems.

1.3. Key Contribution

The critical contributions of this study are extracted as follows:

1. The unknown parameters of the Li-ion battery model are identified in this research using the AVOA;
2. By studying the single-branch Li-ion battery dynamic model, a solid nonlinear connection between the OCV and the SoC is demonstrated;
3. Experiments using Li-ion batteries and simulation-based research are combined;
4. The combination of the CCM and AUKF is compared to other combinations, such as the CCM with EKF, CCM with UKF, and CCM with AEKF;
5. Concerning modeling Li-ion batteries for the SoC estimate, the study filled the gap by excluding loads, battery aging, and temperature conditions.

1.4. Paper Coordination

The remainder of the paper is introduced as follows: Section 2 describes a dynamic demonstration of a Li-ion battery. Section 3 introduces the Coulomb Counting and Adaptive Unscented Kalman Filter methodology. Section 4 reveals the outcome of the hybrid method simulation when applied to solve the issue with the SoC estimation of Li-ion batteries. Section 5 discusses the simulation result and briefs it, and Section 6 outlines the main results of the research.

2. Problem Attributions

In the literature's previous study, nonlinear modeling's impacts were not considered while identifying the battery characteristics and estimating SoC and the effects of noise and measurement errors and their variable uncertainties. The linear model's parameter identification process does not take much time to compute. Conversely, while nonlinear models need more computation time, they can offer good parameter estimate accuracy. Compared to conventional nonlinear models, the recommended approach has created a simpler nonlinear model that offers good identification accuracy with shorter computation times, with accurate SoC estimation that assumes any uncertainties in the error of SoC estimation are variable, not fixed; the model can adapt to any changes. A reduced model with enough precision for parameter estimation must be presented to resolve this problem. This new study's focus is on the previously noted gaps in the literature. A nonlinear depiction of the link between OCV and the SoC is considered because the battery's internal chemical reactions are unstable.

2.1. Modeling of Li-Ion Battery

Different Li-ion battery models were shown and evaluated for their complexity and precision; an ECM for battery with lumped parameters for single and double polarization branches was the better option. The most popular one selected for this work is the single-order branch model, also known as the single-time constant model of Li-ion batteries. The battery is modeled in Figure 1 [30].

This Li-ion battery model consists of a battery OCV (V_{ocv}), series ohmic resistance (R_o), the battery's transient resistance and capacitance (R_{tr}, C_{tr}), and (I_{batt}) is the battery terminal current.

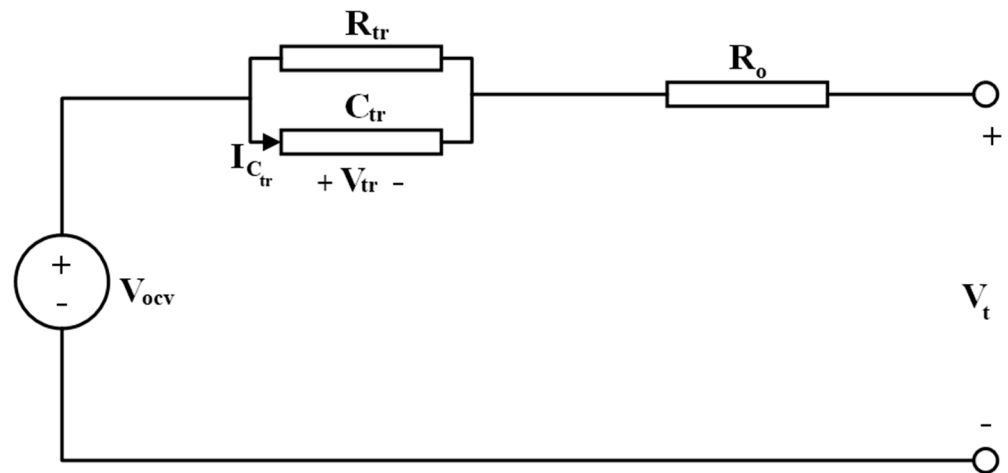


Figure 1. Model of the Li-ion battery [30].

The electric behavior of the single-time constant model may be characterized by Equations (1) and (2):

$$V_{tr}^{\circ} = \frac{-1}{R_{tr} * C_{tr}} V_{tr} + \frac{1}{C_{tr}} I_{batt} \tag{1}$$

$$V_t = V_{ocv} - V_{tr} - R_o * I_{batt} \tag{2}$$

The discrete-time explanation may be seen in Equations (3) and (4) as follows:

$$V_{tr,k+1} = V_{tr,k} e^{\frac{-\tau_s}{\tau_{tr}}} + R_{tr} \left(1 - e^{\frac{-\tau_s}{\tau_{tr}}} \right) I_{batt,k} \tag{3}$$

$$V_{t,k} = V_{ocv} (SoC,k) - V_{tr,k} - R_o * I_{batt,k} \tag{4}$$

where (τ_s) is the sample time and (τ_{tr}) is the tau time constant of the transient branch.

2.2. State of Charge Equations

The battery cell's SoC reveals how much energy is still available in the cell compared to its capacity, as shown in Equation (5).

$$SoC = SoC_0 - \frac{1}{Q} \int_0^t I_{batt} dt \tag{5}$$

where (Q) is the capacity of a Li-ion battery, (SoC_0) is the initial state of charge value, and (I_{batt}) is the load current. Equation (5) is used to compute SoC to determine (V_{ocv}) in Equation (3) and to calculate the terminal voltage (V_t) in Equation (4).

The discretization of Equation (5) is shown in Equation (6):

$$SoC_k = SoC_{k-1} - 100 \frac{I_{batt,k-1}}{3600 * Q} \tag{6}$$

Now using Equations (1)–(4), the equations of the state space of the Li-ion battery model are presented in Equations (7) and (8).

$$\begin{bmatrix} SoC_k \\ V_{tr,k} \end{bmatrix} = \begin{bmatrix} 1 & 0 \\ 0 & e^{\frac{-\tau_s}{R_{tr} C_{tr}}} \end{bmatrix} \begin{bmatrix} SoC_{k-1} \\ V_{tr,k-1} \end{bmatrix} + \begin{bmatrix} -100 \frac{1}{3600 * Q} \\ R_{tr} \left[1 - e^{\frac{-\tau_s}{R_{tr} C_{tr}}} \right] \end{bmatrix} I_{batt,k-1} \tag{7}$$

$$V_t = \begin{bmatrix} -1 \\ 0 \end{bmatrix}^T \begin{bmatrix} V_{tr,k} \\ I_{batt,k} \end{bmatrix} - R_o I_{batt,k} + V_{ocv,k} \tag{8}$$

To brief the process of SoC estimation, Figure 2 demonstrates the SoC estimation framework.

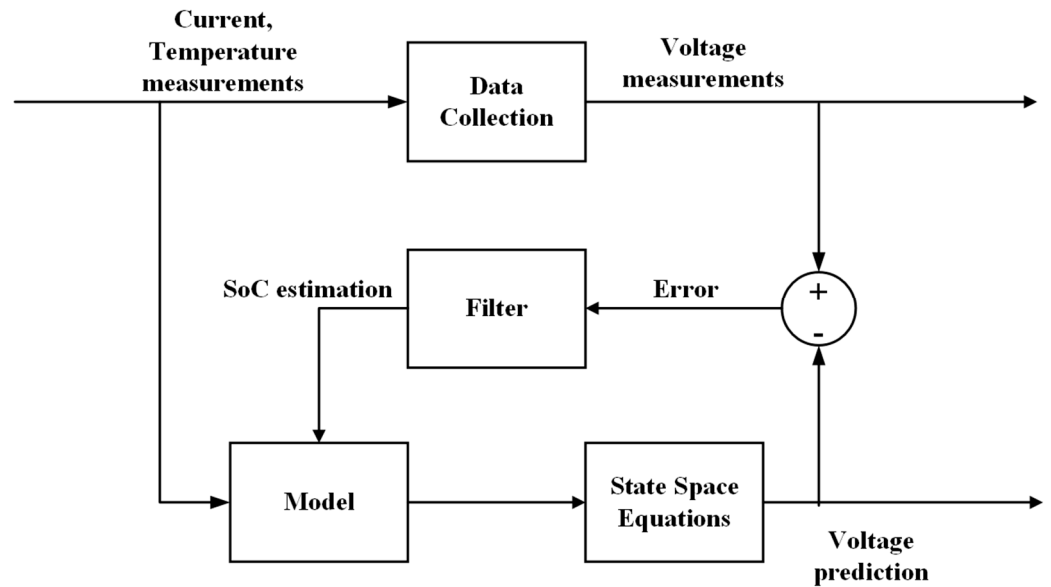


Figure 2. SoC estimation framework.

2.3. Objectives and Constraints of Li-Ion Battery Model SoC Estimation Problem

The single-branch Li-ion battery model discussed in the prior section characterizes the battery characteristics. To match the predicted SoC with the observed state of charge in the experimental step, an objective function must be developed, and SoC must be estimated accurately by using a reliable and accurate estimation method to make sure the Li-ion battery is performing within a safe range, avoiding overcharging and over-discharging problems. The developed objective function is based on decreasing the distinction between the experimental SoC and the simulation results SoC. The proposed objective function is represented in Equation (9).

$$\begin{aligned} &Min_u Fi(u), i = 1, 2, \dots, n_{obj} \\ &Umin \leq U \leq Umax \end{aligned} \tag{9}$$

$F_i(u)$ is the developed goal function, and $(i$ and $u)$ represent the estimated parameters in the battery. The control variables of the parameters are $(Umin)$ and $(Umax)$, and n_{obj} consists of all possible objective functions. Using the results of the Li-ion battery experiment, the parameters of the Li-ion battery model are established.

The goal is to reduce the average discrepancy between the simulated battery and the experimented battery SoC $F_i(u)$ by using Equation (10).

$$F_i(u) = \sum (SoC_{estimated} - SoC_{experimental})^2 \tag{10}$$

where $(SoC_{estimated})$ is the simulated battery SoC and $(SoC_{experimental})$ is the experimental battery SoC.

Under the primary constraints, the objective function is solved:

$$\begin{aligned} &0 \leq SoC \leq 1 \\ &V_{ocv\ min} \leq V_{ocv} \leq V_{ocv\ max} && \text{at } T_1 = 25\ ^\circ\text{C and } T_2 = 45\ ^\circ\text{C} \\ &R_o\ min \leq R_o \leq R_o\ max && \text{at } T_1 = 25\ ^\circ\text{C and } T_2 = 45\ ^\circ\text{C} \\ &R_{tr}\ min \leq R_{tr} \leq R_{tr}\ max && \text{at } T_1 = 25\ ^\circ\text{C and } T_2 = 45\ ^\circ\text{C} \\ &\tau_{tr}\ min \leq \tau_{tr} \leq \tau_{tr}\ max && \text{at } T_1 = 25\ ^\circ\text{C and } T_2 = 45\ ^\circ\text{C} \end{aligned}$$

where (min) and (max) are the parameters' restrictions operators.

3. Coulomb Counting Method and Adaptive Unscented Kalman Filter

3.1. Coulomb Counting Method

According to Kiarash et al. [31], the Coulomb Counting equation is presented in Equation (11).

$$SoC(t) = SoC(0) + \frac{\eta}{3600 Q} \int_0^t i(t) dt \quad (11)$$

where (η) is the Coulomb efficiency which is denoted as follows in Equation (12):

$$\eta = \begin{cases} \eta_{charge}, & i(t) > 0 \\ \eta_{discharge}, & i(t) < 0 \end{cases} \quad (12)$$

where (t) is time in seconds, ($i(t)$) is the current flowing through in the battery amperes (A) at the time (t), ($SoC(t)$) is the SoC at a time interval (t), ($SoC(0)$) is the SoC at time instant ($t = 0$), and (Q) is battery capacity in (Ahr).

After discretizing the Coulomb Counting equation, we obtain Equation (13):

$$SoC(j) = SoC(j-1) + \frac{\eta}{3600 Q} \int_{t(j-1)}^{t(j)} i(\tau) d\tau \quad (13)$$

where ($SoC(j)$) denotes the SoC at time instant ($t(j)$), ($SoC(j-1)$) indicates SoC value at time instant ($t(j-1)$), and ($i(\tau)$) indicates the current measured at time instant (τ). The integration in Equation (14) is approximated using the rectangle (backward difference) approach in Equation (13).

$$\int_{t(j-1)}^{t(j)} i(\tau) d\tau \approx \Delta_j i(t(j)) = \Delta_j i(j) \quad (14)$$

where $\Delta_j = t(j) - t(j-1)$. Equation (15) illustrates the simplified Coulomb Counting equation as follows:

$$SoC(j) = SoC(j-1) + \frac{\eta \Delta_j i(j)}{3600 Q} \quad (15)$$

In Equation (15), the following inaccuracies are present in the Coulomb Counting equation:

1. Current measurement inaccuracy $i(j)$;
2. An error result from the integration's approximation in Equation (14);
3. Knowledge of battery capacity (Q) is unreliable;
4. A lack of understanding regarding the efficiency of Coulomb Counting η ;
5. Sampling time (Δ) measurement error.

Therefore, to limit these errors, the AUKF is initially employed to lead the starting value to the actual value.

3.2. Adaptive Unscented Kalman Filter (AUKF) Methodology

When turning a nonlinear system into a linear system, unscented transformation should be used instead of the Taylor expansion to boost the accuracy of the Unscented Kalman Filter (UKF) approach. Although the noise from the system model and observations in the UKF method is specified as constants, they cannot accurately represent the impact of actual noise on the filter, leading to an increase or even a divergence in the SoC estimate error. The AUKF algorithm, an improved version of the UKF algorithm, addresses the issues above. The algorithm computes the innovation variance and residual variance using the Moving Window approach, and it continuously observes the evolution of innovation and residual in the filter. While the residual variance adjusts the observation noise covariance instantaneously, the innovation variance adjusts the system noise covariance instantaneously [32].

The process of the AUKF is presented as follows:

Step (1): Define the initial state value (\hat{x}_0) and state error covariance initial value (P_0) in Equations (16) and (17).

$$\hat{x}_0 = E[x_0] \tag{16}$$

$$P_0 = E[(x_0 - \hat{x}_0)(x_0 - \hat{x}_0)^T] \tag{17}$$

Step (2): Calculate the Sigma point through Equation (18).

$$\begin{cases} x_j^0 = \hat{x}_{j-1} \\ x_{j-1}^i = \hat{x}_{j-1} + \sqrt{(L + \lambda)P_{j-1}}, \quad i = 1, 2, \dots, L \\ x_{j-1}^i = \hat{x}_{j-1} - \sqrt{(L + \lambda)P_{j-1}}, \quad i = L + 1, L + 2, \dots, 2L \end{cases} \tag{18}$$

where (L) is the state vector length, the calculation of the weight value is presented in Equation (19).

$$\begin{cases} \lambda = \alpha^2(L + j_i) - L \\ W_m^0 = \frac{\lambda}{L + \lambda}, \quad W_m^i = \frac{1}{2(L + \lambda)}, \quad i = 1, 2, \dots, 2L \\ W_c^0 = \frac{\lambda}{L + \lambda} + 1 - \alpha^2 + \beta, \quad W_c^i = \frac{1}{2(L + \lambda)}, \quad i = 1, 2, \dots, 2L \end{cases} \tag{19}$$

Step (3): Time update.

1. Update the value of the predicted status (\bar{x}_j) from Equations (20) and (21).

$$x_{j|j-1}^i = F(x_{j-1}^i) \tag{20}$$

$$\bar{x}_j = \sum_{i=0}^{2L} W_m^i x_j^i \tag{21}$$

2. Update the value of the predicted observation (\bar{y}_j) from Equations (22) and (23).

$$y_{j|j-1}^i = G(x_{j|j-1}^i) \tag{22}$$

$$\bar{y}_j = \sum_{i=0}^{2L} W_m^i [G(x_{j|j-1}^i) + v] = \sum_{i=0}^{2L} W_m^i y_{j|j-1}^i \tag{23}$$

3. Update the predicted value of system covariance ($P_{xx|j}$) from Equation (24).

$$P_{xx|j} = \sum_{i=0}^{2L} (W_c^i (x_{j|j-1}^i - \bar{x}_j)(x_{j|j-1}^i - \bar{x}_j)^T) + Q_{j-1} \tag{24}$$

4. Calculate innovative value (d_j) and innovative variance value (C_{d_j}) from Equations (25) and (26).

$$d_j = y_j - \bar{y}_j \tag{25}$$

$$C_{d_j} = \begin{cases} \frac{j-1}{j} C_{d_{j-1}} + \frac{1}{j} d_j d_j^T, & j \leq W \\ \frac{1}{W} \sum_{i=j-W+1}^j d_i d_i^T, & j > W \end{cases} \tag{26}$$

- Update system noise covariance (Q_j) from Equation (27).

$$Q_j = K_{j-1} C_{d_j} K_{j-1}^T \quad (27)$$

Step (4): A status update.

- Update the prediction value of observation covariance ($P_{yy|j}$) from Equation (28).

$$P_{yy|j} = \sum_{i=0}^{2L} (W_c^i (y_{j|j-1}^i - \bar{y}_j) (y_{j|j-1}^i - \bar{y}_j)^T) + R_{j-1} \quad (28)$$

- Update covariance ($P_{xy|j}$) from Equation (29).

$$P_{xy|j} = \sum_{i=0}^{2L} W_c^i (x_{j|j-1}^i - \bar{x}_j) (y_{j|j-1}^i - \bar{y}_j)^T \quad (29)$$

- Calculate Kalman gain from Equation (30).

$$K_j = \frac{P_{xy|j}}{P_{yy|j}} \quad (30)$$

- Update the value of the estimated state (\hat{x}_j) from Equation (31).

$$\hat{x}_j = \bar{x}_j + K_j (y_j - \bar{y}_j) \quad (31)$$

- Update the value of the estimated observation (\hat{y}_j) from Equation (32).

$$\hat{y}_j = H_j \hat{x}_j \quad (32)$$

- Update the value of error covariance (P_j) from Equation (33).

$$P_j = P_{xx|j} - K_j P_{yy|j} K_j^T \quad (33)$$

- Calculate the value of the residual (r_j) and the value of residual variance (C_{r_j}) in Equations (34) and (35).

$$r_j = y_j - \hat{y}_j \quad (34)$$

$$C_{r_j} = \begin{cases} \frac{j-1}{j} C_{d_{r-1}} + \frac{1}{j} r_j r_j^T, & j \leq W \\ \frac{1}{W} \sum_{i=j-W+1}^j r_i r_i^T, & j > W \end{cases} \quad (35)$$

- Update the value of the observation noise covariance (R_j) from Equation (36).

$$R_j = C_{r_j} + H_j P_j H_j^T \quad (36)$$

3.2.1. System Noise Covariance of Adaptive System (Q_j)

The previous equations prove that when (Q_j) is very large, system covariance prediction ($P_{xx|j}$) increases, therefore, state value (\bar{x}_{j+1}) increases, which leads to a high value of the predicted state (\widehat{x}_{j+1}), therefore increasing the error of the estimated state of charge. Covariance of system noise (Q_j) will be updated instantaneously to correct the effect of system errors on estimated results.

The difference between the actual observation value (y_j) and the value of predicted observation (\hat{y}_j) is denoted as innovation (d_j) at the time (j), which is shown in Equation (25).

In the Moving Window method, innovation variance (C_{d_j}) is denoted in Equation (26). Where (W) is the Moving Window length from the innovative variance (C_{d_j}) equation, the system noise covariance (Q_j) is calculated from Equation (37).

$$Q_j = K_{j-1} C_{d_{j-1}} K_{j-1}^T \quad (37)$$

Therefore, by calculating the innovation value (d_j) and updating (Q_j) instantaneously to correct the covariance error (P_j), the value of system noise is corrected, and the (Q_j) reaches zero.

3.2.2. Observation Noise Covariance of Adaptive System (R_j)

The previous equations denote that (R_j) establishes the importance of the observation value with the estimated outcome. As (R_j) increases, Kalman gains (K_j) decrease, which causes the observation value to have a negligible impact on the predicted state value. Similarly, as (R_j) decreases, filter gain (K_j) increases, which causes the observation value to have a significant impact on the predicted state value. Therefore, the covariance of observation noise (R_j) reduces the impact of observation noise on estimating results by adjusting the Kalman gain (K_j) instantaneously to modify the impact of the observation predicted value.

The residual (r_j) at a time (j), which is displayed in Equation (34), is the divergence between the actual value (y_j) and the estimated value of observation (\hat{y}_j).

In the Moving Window method, the value of the variance of residual (C_{r_j}) is denoted in Equation (38).

$$C_{r_j} = \begin{cases} \frac{j-1}{j} C_{r_{j-1}} + \frac{1}{j} r_j r_j^T, & j \leq W \\ \frac{1}{W} \sum_{i=j-W+1}^j r_i r_i^T, & j > W \end{cases} \quad (38)$$

From the value of residual variance (C_{r_j}) equation, the value of observation noise covariance (R_j) is calculated from Equation (39).

$$R_j = C_{r_j} + H_j P_{j-1} H_j^T \quad (39)$$

Therefore, by calculating the residual value (r_j) and updating (R_j) in real-time and adjusting Kalman gain (K_j), we can achieve optimal estimation.

To brief this section, Figure 3 illustrates the AUKF flowchart.

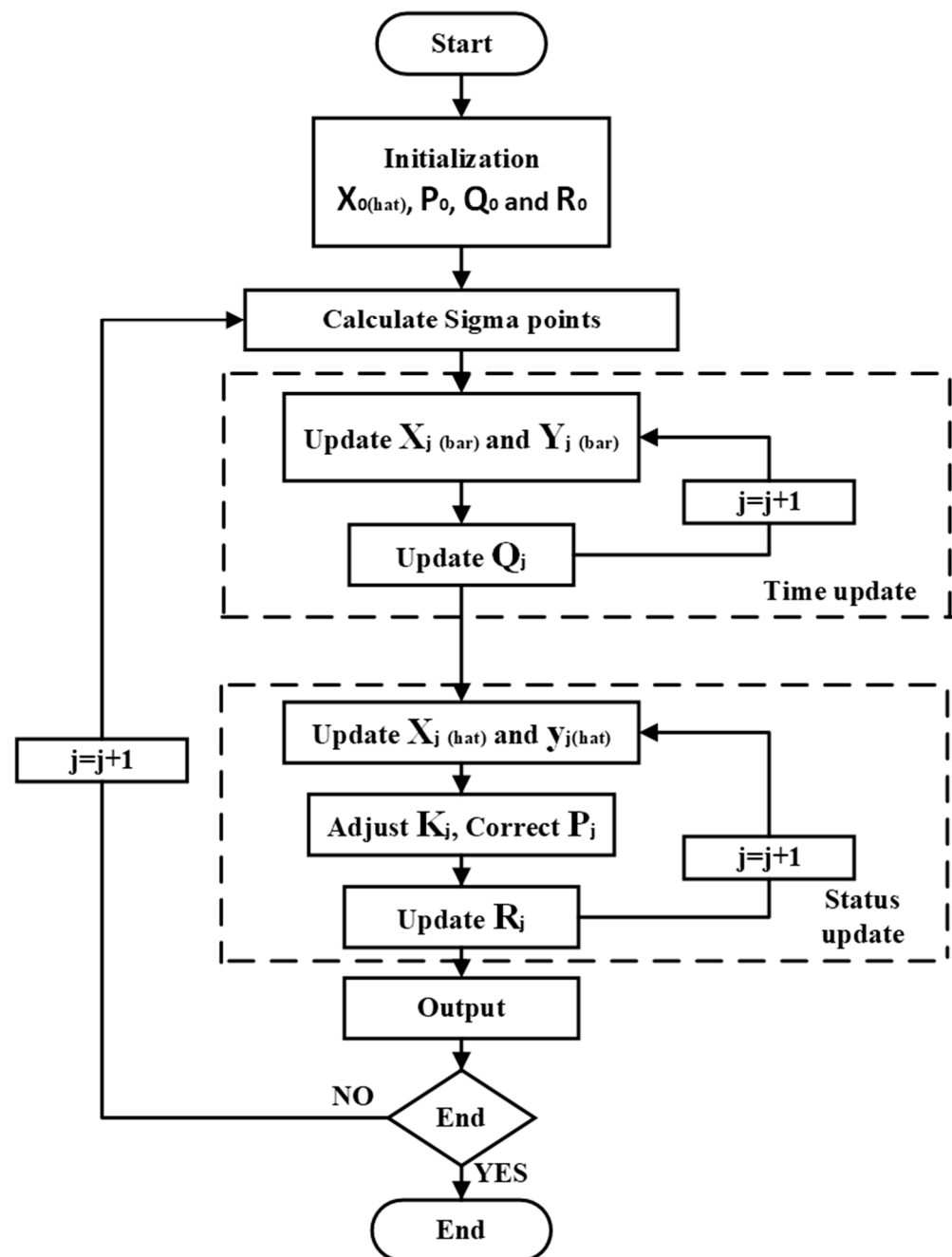


Figure 3. The AUKF flowchart.

4. Experimental Results

This section presents a rechargeable Li-ion battery, 3.7 V, 2.6 Ah, as it has strong performance and dependability. Its characteristics include the following details in Tables 1–3 [30].

Other constants are considered while simulating the Li-ion battery, represented in Table 2.

Four approaches are applied for Li-ion batteries as follows:

1. Approach (1): resistive load and battery fade are not considered;
2. Approach (2): battery fade is considered, but the resistive load is not;
3. Approach (3): resistive load is included; battery fade is not;
4. Approach (4): resistive and battery fade are considered.

Table 1. Li-ion battery characteristics.

Battery	Value
Average Voltage (V_{nom})	3.7
Least Capacity (Ah)	2.45
Ideal Capacity (Ah)	2.6
Series Resistance (Ω)	0.05
Maximum Charging/Discharging Current (A)	2/2
Charging CC/CV (mA, V)	1750, 4.20
Charging Time (h)	3
Ambient Temperature ($^{\circ}\text{C}$)	Charging Temperature: (0~+45 $^{\circ}\text{C}$) Discharging Temperature: (-20~+60 $^{\circ}\text{C}$)
Weight (g)	48

Table 2. Li-ion battery constants.

Parameter	Value
Discharge capacity (Q_{dis}) (Ahr)	1.4
No discharge cycles (N)	100
Capacity (Q_{fade}) after (N) discharge cycles (Ahr)	2
(R_o) after (N) discharge cycles (Ω)	0.15
(V_{dis}) after (N) discharge cycles (V)	3
No population size	20
No of iterations	500
The initial state of charge (SoC_0)	0.5
Charging and discharging time (s)	21,600
Series resistance initial values (used for AUKF) (Ω)	0.05
Initial state error covariance (P_0)	$[1 \times 10^{-6} \ 0; \ 0 \ 1]$
Measurement noise covariance (R)	0.25
Process noise covariance (Q)	$[1 \times 10^{-1} \ 0; \ 0 \ 1 \times 10^{-1}]$
Alpha (α)	1
Beta (β)	1
Kappa (κ)	0

Table 3. Li-ion battery parameters' boundaries.

Parameter	At $T_1 = 25^{\circ}\text{C}$		Parameter	At $T_2 = 45^{\circ}\text{C}$	
	LB	UB		LB	UB
V_{nom} (V)	3	4	V_{nom} (V)	3	4
$R_o T_1$ (Ω)	0.045	0.06	$R_o T_2$ (Ω)	0.07	0.085
$R_{tr} T_1$ (Ω)	0.005	0.015	$R_{tr} T_2$ (Ω)	0.007	0.01
$\tau_{tr} T_1$ (s)	100	200	$\tau_{tr} T_2$ (s)	150	250

4.1. Simulation of Approach (1)

In this approach, both loading and battery fade effects are excluded. Table 4 represents the values of optimized parameters by using African Vultures Optimization Algorithm (AVOA) at different state of charge values at temperatures 25 $^{\circ}\text{C}$ and 45 $^{\circ}\text{C}$; then, after estimating the SoC, Table 5 represents the SoC error (ISE) which is utilized in curves between the contrasted hybrid approaches in Figure 4.

Table 4. Approach (1): optimized parameters of the Li-ion battery at different SoC values.

	SoC = 0	SoC = 0.1	SoC = 0.25	SoC = 0.5	SoC = 0.75	SoC = 0.9	SoC = 1
$V_{nom} T_1$	3	3.06	3.13	3.22	3.42	3.58	3.7
$R_o T_1$	0.0515	0.0508	0.0512	0.0519	0.0519	0.0525	0.0528
$R_{tr} T_1$	0.0137	0.0097	0.0075	0.0062	0.0061	0.0061	0.0056
$\tau_{tr} T_1$	104.65	115.36	193.45	120.54	143.71	124.36	109.71
$V_{nom} T_2$	3.2109	3.2812	3.3409	3.4269	3.6409	3.7954	3.9009
$R_o T_2$	0.0801	0.0801	0.0803	0.0798	0.0799	0.08	0.08
$R_{tr} T_2$	0.0083	0.0078	0.008	0.0079	0.0086	0.0081	0.008
$\tau_{tr} T_2$	157	166	226	150	198	154	160

Table 5. Approach (1): Li-ion battery SoC error using comparative hybrid techniques.

	CC + EKF	CC + UKF	CC + AEKF	CC + AUKF
<i>ISE</i>	0.000285955	8.58843×10^{-5}	5.80235×10^{-5}	1.72978×10^{-6}

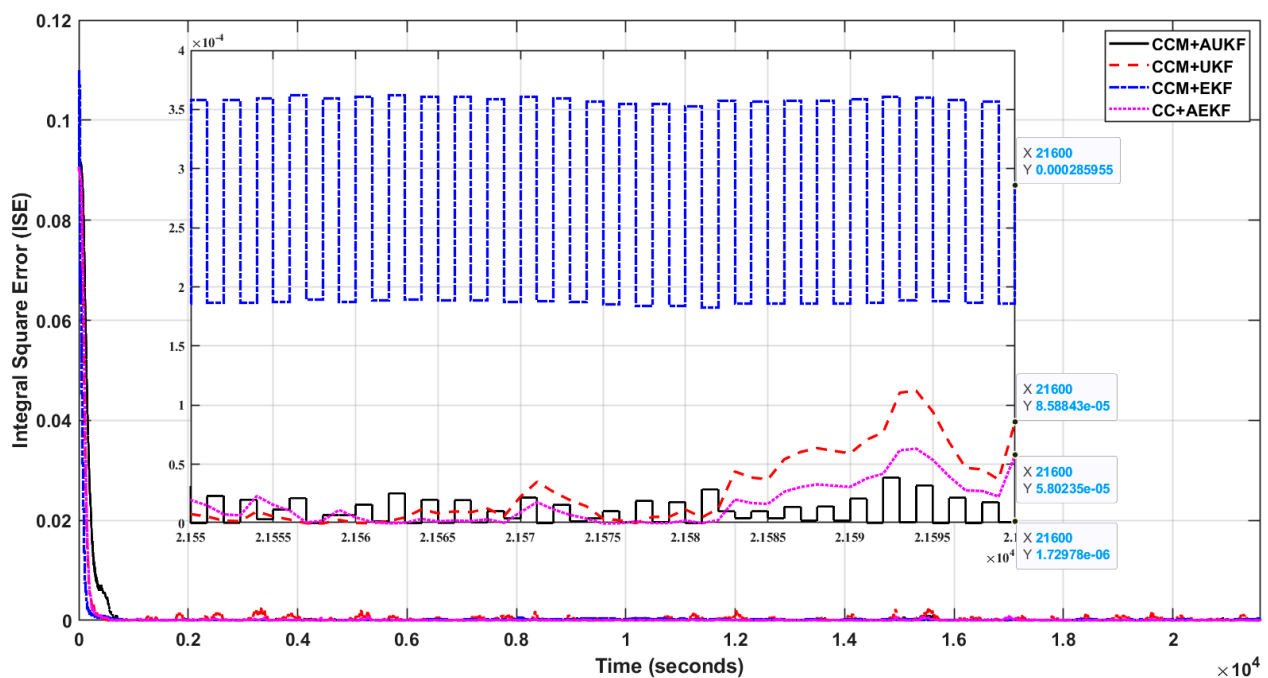
**Figure 4.** Convergence curves for the Li-ion battery for Approach (1).

Figure 4 reveals the convergence curves between the integral square error (*ISE*) and time in seconds.

4.2. Simulation of Approach (2)

In this approach, the effect of battery fading is included, while loading is not included. Both battery capacity and battery series resistance are affected by aging. Resistance increases are caused by several causes, including developing (SEI) at the corrosion of the current collector's anode, cathode, and interfaces. These mechanisms cause battery fading and are influenced by temperature, charge state, and storage time. Table 6 represents the values of optimized parameters by using the African Vultures Optimization Algorithm (AVOA) at different state of charge values at temperatures 25 °C and 45 °C; then, after estimating the SoC, Table 7 represents the SoC error (*ISE*), which is utilized in curves between the contrasted hybrid approaches in Figure 5.

Table 6. Approach (2): optimized parameters of the Li-ion battery at different SoC values.

	SoC = 0	SoC = 0.1	SoC = 0.25	SoC = 0.5	SoC = 0.75	SoC = 0.9	SoC = 1
$V_{nom} T_1$	3.024	3.084	3.154	3.244	3.444	3.604	3.724
$R_o T_1$	0.0496	0.0489	0.0493	0.050	0.052	0.0526	0.0529
$R_{tr} T_1$	0.00992	0.00952	0.00732	0.00602	0.00592	0.00592	0.00542
$\tau_{tr} T_1$	104.5687	115.9845	193.4587	120.3648	143.5681	124.5847	109.2108
$V_{nom} T_2$	3.231	3.301	3.361	3.441	3.661	3.811	3.9210
$R_o T_2$	0.08436	0.08436	0.08456	0.08406	0.08416	0.08426	0.08426
$R_{tr} T_2$	0.00885	0.00835	0.00855	0.00845	0.00915	0.00865	0.00855
$\tau_{tr} T_2$	157.412	166.785	226.457	150.251	198.473	154.785	160.251

Table 7. Approach (2): Li-ion battery SoC error using comparative hybrid techniques.

	CC + EKF	CC + UKF	CC + AEKF	CC + AUKF
ISE	0.000297115	0.000260252	4.28443×10^{-5}	2.78046×10^{-5}

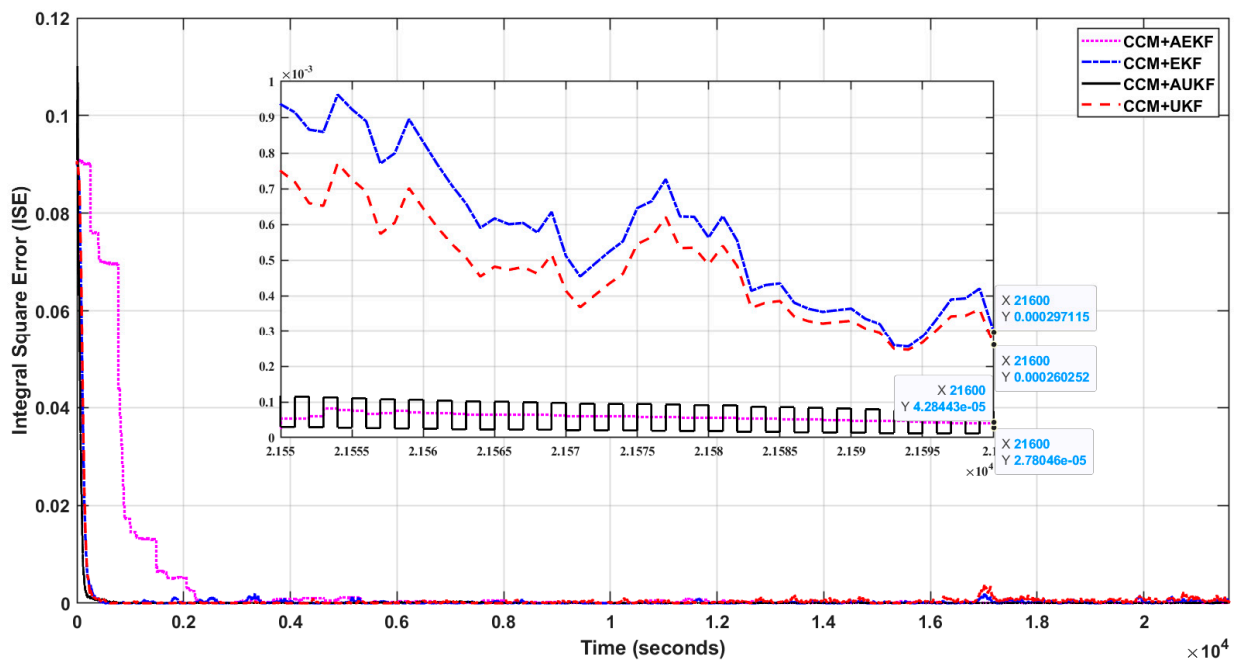


Figure 5. Convergence curves for Li-ion battery for Approach (2).

Figure 5 reveals the convergence curves between the integral square error (ISE) and time in seconds.

4.3. Simulation of Approach (3)

In this approach, a resistive load equal to 1 kΩ is studied while the battery fade is not. Table 8 represents the values of optimized parameters by using the African Vultures Optimization Algorithm (AVOA) at different SoC values at temperatures 25 °C and 45 °C; then, after estimating the SoC, Table 9 represents the SoC error (ISE) which is utilized in curves between the contrasted hybrid approaches in Figure 6.

Table 8. Approach (3): optimized parameters of the Li-ion battery at different SoC values.

	SoC = 0	SoC = 0.1	SoC = 0.25	SoC = 0.5	SoC = 0.75	SoC = 0.9	SoC = 1
$V_{nom} T_1$	3.0115	3.0715	3.1415	3.2315	3.4315	3.5915	3.7115
$R_o T_1$	0.05115	0.05045	0.05085	0.05155	0.05155	0.05215	0.05245
$R_{tr} T_1$	0.00982	0.00942	0.00722	0.00592	0.00572	0.00572	0.00522
$\tau_{tr} T_1$	104.5129	115.3211	193.2314	120.4785	143.9845	124.9541	109.1172
$V_{nom} T_2$	3.2213	3.2913	3.3513	3.4313	3.6513	3.8013	3.9113
$R_o T_2$	0.0842	0.0846	0.0848	0.0843	0.0844	0.08450	0.08452
$R_{tr} T_2$	0.00891	0.00841	0.00861	0.00861	0.00931	0.00881	0.00871
$\tau_{tr} T_2$	157.8632	166.8732	226.1234	150.3648	198.4155	154.2844	160.8211

Table 9. Approach (3): Li-ion battery SoC error using comparative hybrid techniques.

	CC + EKF	CC + UKF	CC + AEKF	CC + AUKF
ISE	5.82592×10^{-5}	0.000256599	8.53238×10^{-5}	1.52231×10^{-6}

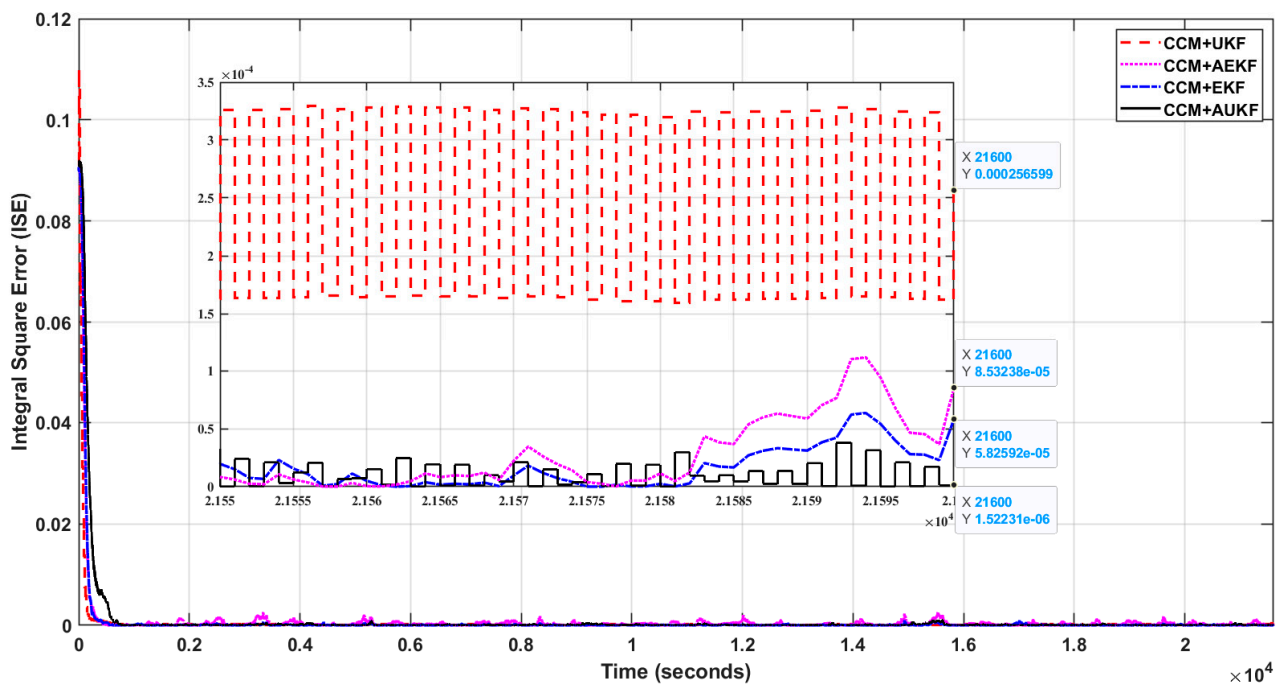


Figure 6. Convergence curves for Li-ion battery for Approach (3).

Figure 6 reveals the convergence curves between the integral square error (ISE) and time in seconds.

4.4. Simulation of Approach (4)

In this approach, both the resistive load and battery fade are considered. Table 10 represents the values of optimized parameters by using the African Vultures Optimization Algorithm (AVOA) at different state of charge values at temperatures 25 °C and 45 °C; then, after estimating the SoC, Table 11 represents the SoC error (ISE) which is utilized in curves between the contrasted hybrid approaches in Figure 7.

Table 10. Approach (4): optimized parameters of the Li-ion battery at different SoC values.

	SoC = 0	SoC = 0.1	SoC = 0.25	SoC = 0.5	SoC = 0.75	SoC = 0.9	SoC = 1
$V_{nom} T_1$	3.011	3.071	3.141	3.231	3.431	3.591	3.711
$R_o T_1$	0.0523	0.0514	0.0517	0.0522	0.0522	0.0528	0.0531
$R_{tr} T_1$	0.00891	0.00931	0.00711	0.00581	0.00571	0.00561	0.00521
$\tau_{tr} T_1$	104.3675	115.2178	193.3245	120.6478	143.86321	124.9541	109.1131
$V_{nom} T_2$	3.2101	3.2801	3.3401	3.4201	3.6401	3.7901	3.9001
$R_o T_2$	0.0858	0.0858	0.086	0.0855	0.0857	0.0858	0.0861
$R_{tr} T_2$	0.008275	0.007875	0.008075	0.007975	0.008675	0.008275	0.008175
$\tau_{tr} T_2$	157.3211	166.3222	226.3144	150.3644	198.2345	154.2387	160.7111

Table 11. Approach (4): Li-ion battery SoC error using comparative hybrid techniques.

	CC + EKF	CC + UKF	CC + AEKF	CC + AUKF
ISE	0.000259489	0.000298199	5.85516×10^{-5}	4.44024×10^{-5}

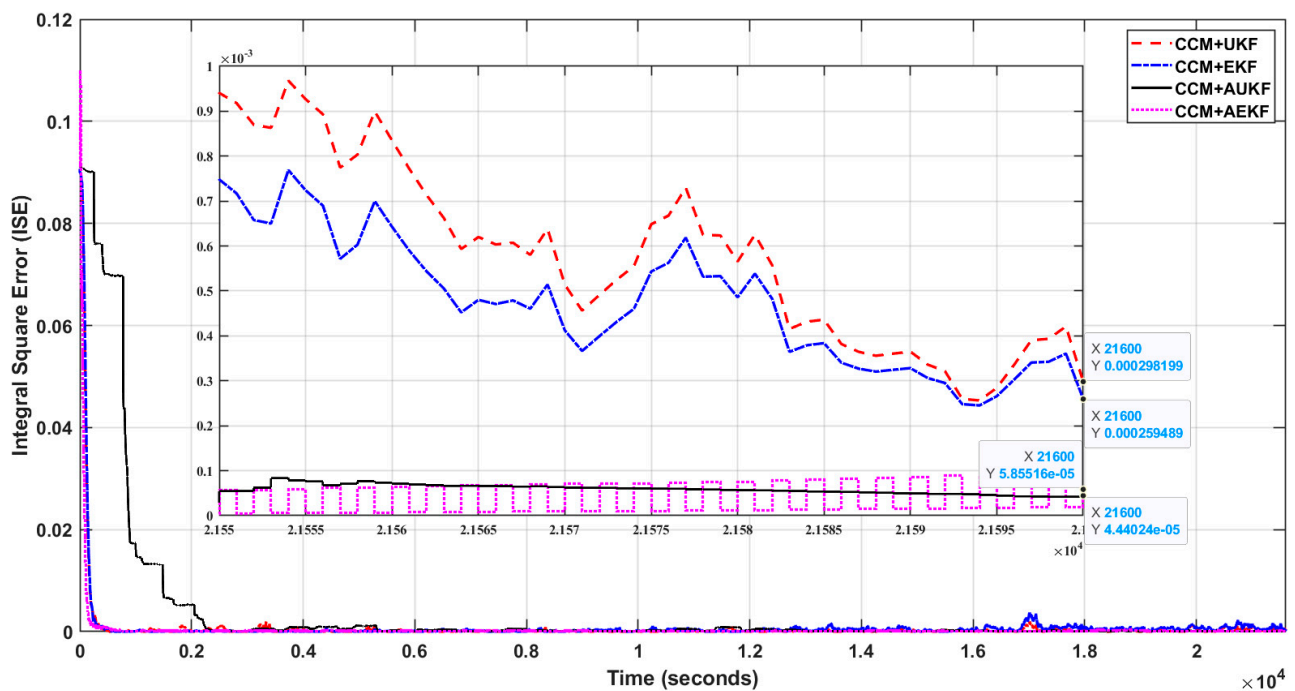
**Figure 7.** Convergence curves for Li-ion battery for Approach (4).

Figure 7 reveals the convergence curves between the integral square error (*ISE*) and time in seconds.

5. Discussion

This study explains the connection between the battery characteristics and SoC at different loading, temperatures, and aging conditions; by comparing to other studies, the results prove the reduction of the error between the estimated SoC and real SoC by using a new hybrid method which is a combination of the CCM and AUKF. Tables 12–15 demonstrate the Li-ion battery's attained objective value under contrasting techniques.

Table 12. Li-ion battery objective value using hybrid comparative techniques for Approach (1).

	CC + EKF	CC + UKF	CC + AEKF	CC + AUKF
ISE	0.000285955	8.58843×10^{-5}	5.80235×10^{-5}	1.72978×10^{-6}
Rank	4 (<i>Max.</i>)	3	2	1 (<i>Min.</i>)

Table 13. Li-ion battery objective value using hybrid comparative techniques for Approach (2).

	CC + EKF	CC + UKF	CC + AEKF	CC + AUKF
ISE	0.000267115	0.000260252	4.28443×10^{-5}	2.78046×10^{-5}
Rank	4 (<i>Max.</i>)	3	2	1 (<i>Min.</i>)

Table 14. Li-ion battery objective value using hybrid comparative techniques for Approach (3).

	CC + EKF	CC + UKF	CC + AEKF	CC + AUKF
ISE	5.82592×10^{-5}	0.000256599	8.53238×10^{-5}	1.52231×10^{-6}
Rank	2	4 (<i>Max.</i>)	3	1 (<i>Min.</i>)

Table 15. Li-ion battery objective value using hybrid comparative techniques for Approach (4).

	CC + EKF	CC + UKF	CC + AEKF	CC + AUKF
ISE	0.000259489	0.000298199	5.85516×10^{-5}	4.44024×10^{-5}
Rank	3	4 (<i>Max.</i>)	2	1 (<i>Min.</i>)

As explained in Tables 12–15, based on the value of the error and convergence curve, the CCM with AUKF gives the minimum (ISE) and best behavior for the convergence curve in all approaches.

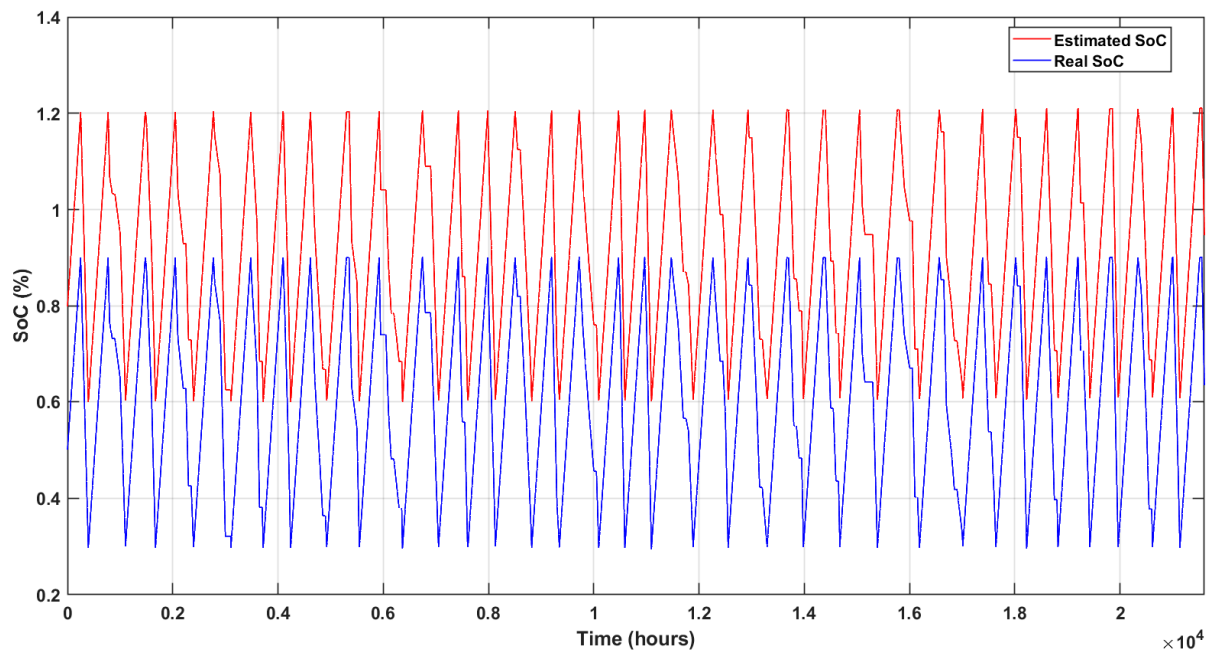
For more confirmation that the hybrid method fits as the best SoC estimation technique and has the least error, using every estimation method as an individual without including any hybrid techniques gives a larger error than using the hybrid technique. Table 16 demonstrates the outcomes of applying various SoC estimate methods on Li-ion batteries for all approaches.

Table 16. SoC error values in all approaches using individual estimating methods.

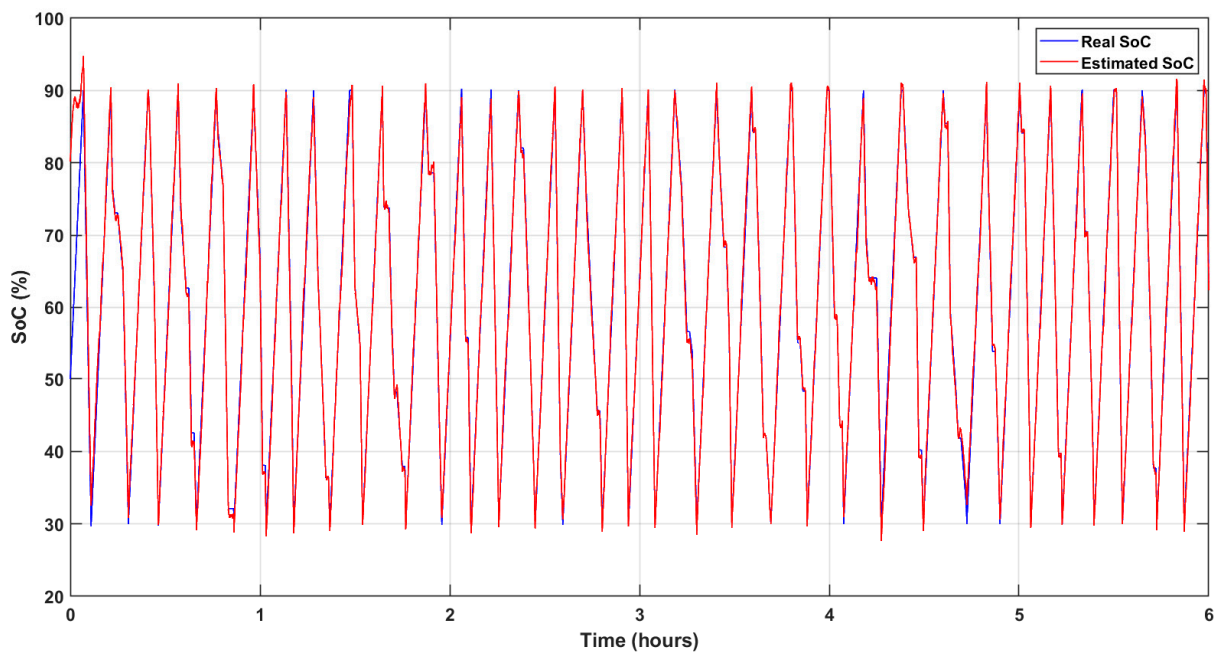
	Approach (1)	Approach (2)	Approach (3)	Approach (4)
CCM	0.0924891	0.0959956	0.0979244	0.101549
EKF	0.000537848	0.00036549	0.000543256	0.000453648
UKF	1.23475×10^{-4}	3.24046×10^{-4}	0.000235487	0.000397456
AEKF	2.47858×10^{-5}	0.000215894	4.23578×10^{-5}	8.34568×10^{-5}
AUKF	3.47268×10^{-5}	5.47866×10^{-5}	1.5431×10^{-5}	8.82024×10^{-5}

As we compare the results, the hybrid method gives a more optimal estimation for SoC. Another verification for using an optimal estimating technique is comparing real and estimated SoC curves, as shown in Figure 8.

As shown in Figure 8a, the battery suffered from (± 0.2) overcharging, which will affect the battery lifetime, and in long distances, the lifetime of the internal parts will be decreased and damaged. As shown in Figure 8b, while using an accurate battery model by using an accurate optimization technique to model the battery accurately and then using a dependable battery SoC estimation technique, the data are very close to each other.



(a)



(b)

Figure 8. (a) Estimated SoC and experimental SoC before using an accurate model and estimation technique. (b) Estimated SoC and experimental SoC after using an accurate model and estimation technique.

6. Conclusions

This work employed a hybrid approach to calculate the SoC of Li-ion batteries. First, the battery is modeled accurately for accurate SoC estimation by using the African Vultures Optimizer (AVOA), which is considered one of the most effective optimization techniques in modeling a nonlinear model such as the Li-ion battery. Then, the hybrid method consisting of the CCM with the AUKF is used for SoC estimation. AUKF is initially employed to lead the starting value to the actual value and eliminate any error at the first readings, and then Coulomb Counting continues to estimate SoC for a long working time. This hybrid method

is compared to other hybrid methods, such as the CCM with an EKF, CCM with a UKF, and CCM with an AEKF. For the 2.6 Ahr Li-ion battery, the simulation results show that the proposed combination of CCM with AUKF has outstanding dynamic validation and capacity in all situations. The fitness function, when compared to other hybrid approaches, achieves the lowest value by utilizing the most dependable and efficient solution, resulting in high accuracy and minimal errors.

Author Contributions: R.A.S. and H.M.H.: conceptualization and methodology; H.M.F.: validation, formal analysis; H.M.H., R.A.S. and M.A.: investigation, visualization, supervision; J.L.M. and F.J.: validation, review, and editing. All authors have read and agreed to the published version of the manuscript.

Funding: This work was supported by King Saud University, Riyadh, Saudi Arabia.

Data Availability Statement: Not applicable.

Acknowledgments: This work was supported by the Researchers Supporting Project number (RSP2023R467), King Saud University, Riyadh, Saudi Arabia.

Conflicts of Interest: There is no conflict of interest.

Nomenclature

List of symbols and nomenclature

Symbol	Description
SoC	Battery State of Charge
ESS	Energy Storage Systems
BMS	Battery Management System
ISE	Integral Square Error
ECM	Equivalent Circuit Model
OCV	Open-Circuit Voltage
CCM	Coulomb Counting Method
EKF	Extended Kalman Filter
UKF	Unscented Kalman Filter
AKF	Adaptive Kalman Filter
AEKF	Adaptive Extended Kalman Filter
AUKF	Adaptive Unscented Kalman Filter
AVOA	African Vultures Optimization Algorithm
EMF	Electromotive Force
UB	Upper Bound
LB	Lower Bound
SEI	Solid Electrolyte Interfaces
Ah	Ampere-Hour
SoC_0	The initial value of the state of charge
V_{ocv}	Battery Open circuit voltage
R_o	The series battery resistance
R_{tr}	Battery transient resistance
C_{tr}	Battery transient capacitance
V_{tr}	The voltage across the polarization branch of the battery
I_{Ctr}	Current flows in polarization capacitance of the battery
I_{batt}	Battery terminal current
τ_s	Sampling time
τ_{tr}	Transient time constant
V_{nom}	Battery nominal voltage
V_{dis}	Battery discharge voltage

Q	Battery nominal capacity
Q_{dis}	Battery discharge capacity
V_t	Battery terminal voltage
n	Total number of discharge cycles
N	Number of discharge cycles
$F_i(U)$	Objective function
n_{obf}	Number of goal functions
U_{min}, U_{max}	Parameter bounds for the control variable factor
$SoC_{measured}$	Expected battery model state of charge
$SoC_{experimental}$	Recorded experimental battery state of charge
Q_{min}, Q_{max}	Maximum and minimum values of (Q)
$R_{o,min}, R_{o,max}$	Maximum and minimum values of (R_o)
$R_{tr,min}, R_{tr,max}$	Maximum and minimum values of (R_{tr})
$\tau_{tr,min}, \tau_{tr,max}$	Maximum and minimum values of (τ_{tr})
η	Coulomb counting efficiency
α	The alpha coefficient controls the emergence of sigma points and minimizes the error of approximation.
β	The beta coefficient controls the emergence of sigma points and minimizes the error of approximation.
W	Moving window length

References

- Dagal, I.; Akın, B.; Akboy, E. A novel hybrid series salp particle Swarm optimization (SSPSO) for standalone battery charging applications. *Ain Shams Eng. J.* **2022**, *13*, 101747. [[CrossRef](#)]
- Awadallah, M.A.; Venkatesh, B. Accuracy improvement of SOC estimation in lithium-ion batteries. *J. Energy Storage* **2016**, *6*, 95–104. [[CrossRef](#)]
- Sheng, C.; Fu, J.; Li, D.; Jiang, C.; Guo, Z.; Li, B.; Lei, J.; Zeng, L.; Deng, Z.; Fu, X.; et al. Energy management strategy based on health state for a PEMFC/Lithium-ion batteries hybrid power system. *Energy Convers. Manag.* **2022**, *271*, 116330. [[CrossRef](#)]
- Liu, S.; Deng, D.; Wang, S.; Luo, W.; Takyi-Aninakwa, P.; Qiao, J.; Li, S.; Jin, S.; Hu, C. Dynamic adaptive square-root unscented Kalman filter and rectangular window recursive least square method for the accurate state of charge estimation of lithium-ion batteries. *J. Energy Storage* **2023**, *67*, 107603. [[CrossRef](#)]
- Wang, C.; Zhang, X.; Yun, X.; Fan, X. A novel hybrid machine learning coulomb counting technique for state of charge estimation of lithium-ion batteries. *J. Energy Storage* **2023**, *63*, 107081. [[CrossRef](#)]
- Nian, P.; Shuzhi, Z.; Xiongwen, Z. Co-estimation for capacity and state of charge for lithium-ion batteries using improved adaptive extended Kalman filter. *J. Energy Storage* **2021**, *40*, 102559. [[CrossRef](#)]
- Khan, H.F.; Hanif, A.; Ali, M.U.; Zafar, A. A Lagrange multiplier and sigma point Kalman filter based fused methodology for online state of charge estimation of lithium-ion batteries. *J. Energy Storage* **2021**, *41*, 102843. [[CrossRef](#)]
- Khawaja, Y.; Shankar, N.; Qiqieh, I.; Alzubi, J.; Alzubi, O.; Nallakaruppan, M.; Padmanaban, S. Battery management solutions for li-ion batteries based on artificial intelligence. *Ain Shams Eng. J.* **2023**, 102213. [[CrossRef](#)]
- Hao, X.; Wang, S.; Fan, Y.; Xie, Y.; Fernandez, C. An improved forgetting factor recursive least square and unscented particle filtering algorithm for accurate lithium-ion battery state of charge estimation. *J. Energy Storage* **2023**, *59*, 106478. [[CrossRef](#)]
- Chen, Z.; Zhao, H.; Shu, X.; Zhang, Y.; Shen, J.; Liu, Y. Synthetic state of charge estimation for lithium-ion batteries based on long short-term memory network modeling and adaptive H-Infinity filter. *Energy* **2021**, *228*, 120630. [[CrossRef](#)]
- Qiao, J.; Wang, S.; Yu, C.; Yang, X.; Fernandez, C. A chaotic firefly—Particle filtering method of dynamic migration modeling for the state-of-charge and state-of-health co-estimation of a lithium-ion battery performance. *Energy* **2023**, *263*, 126164. [[CrossRef](#)]
- Zheng, Y.; Ouyang, M.; Han, X.; Lu, L.; Li, J. Investigating the error sources of the online state of charge estimation methods for lithium-ion batteries in electric vehicles. *J. Power Sources* **2018**, *377*, 161–188. [[CrossRef](#)]
- Jiang, C.; Wang, S.; Wu, B.; Fernandez, C.; Xiong, X.; Coffie-Ken, J. A state-of-charge estimation method of the power lithium-ion battery in complex conditions based on adaptive square root extended Kalman filter. *Energy* **2020**, *219*, 119603. [[CrossRef](#)]
- Wu, M.; Qin, L.; Wu, G.; Huang, Y.; Shi, C. State of Charge Estimation of Power Lithium-ion Battery Based on a Variable Forgetting Factor Adaptive Kalman Filter. *J. Energy Storage* **2021**, *41*, 102841. [[CrossRef](#)]
- Wu, J.; Fang, C.; Jin, Z.; Zhang, L.; Xing, J. A multi-scale fractional-order dual unscented Kalman filter based parameter and state of charge joint estimation method of lithium-ion battery. *J. Energy Storage* **2022**, *50*, 104666. [[CrossRef](#)]
- Liu, X.; Li, K.; Wu, J.; He, Y.; Liu, X. An extended Kalman filter based data-driven method for state of charge estimation of Li-ion batteries. *J. Energy Storage* **2021**, *40*, 102655. [[CrossRef](#)]
- Tian, Y.; Dong, Q.; Tian, J.; Li, X.; Li, G.; Mehran, K. Capacity estimation of lithium-ion batteries based on optimized charging voltage section and virtual sample generation. *Appl. Energy* **2023**, *332*, 120516. [[CrossRef](#)]

18. Zhang, Z.; Jiang, L.; Zhang, L.; Huang, C. State-of-charge estimation of lithium-ion battery pack by using an adaptive extended Kalman filter for electric vehicles. *J. Energy Storage* **2021**, *37*, 102457. [[CrossRef](#)]
19. Wu, M.; Qin, L.; Wu, G. State of charge estimation of power lithium-ion battery based on an adaptive time scale dual extend Kalman filtering. *J. Energy Storage* **2021**, *39*, 102535. [[CrossRef](#)]
20. Ye, Y.; Li, Z.; Lin, J.; Wang, X. State-of-charge estimation with adaptive extended Kalman filter and extended stochastic gradient algorithm for lithium-ion batteries. *J. Energy Storage* **2021**, *47*, 103611. [[CrossRef](#)]
21. Tian, Y.; Lai, R.; Li, X.; Xiang, L.; Tian, J. A combined method for state-of-charge estimation for lithium-ion batteries using a long short-term memory network and an adaptive cubature Kalman filter. *Appl. Energy* **2020**, *265*, 114789. [[CrossRef](#)]
22. Zhu, R.; Duan, B.; Zhang, J.; Zhang, Q.; Zhang, C. Co-estimation of model parameters and state-of-charge for lithium-ion batteries with recursive restricted total least squares and unscented Kalman filter. *Appl. Energy* **2020**, *277*, 115494. [[CrossRef](#)]
23. Shi, N.; Chen, Z.; Niu, M.; He, Z.; Wang, Y.; Cui, J. State-of-charge estimation for the lithium-ion battery based on adaptive extended Kalman filter using improved parameter identification. *J. Energy Storage* **2021**, *45*, 103518. [[CrossRef](#)]
24. Miao, Y.; Gao, Z. Estimation for state of charge of lithium-ion batteries by adaptive fractional-order unscented Kalman filters. *J. Energy Storage* **2022**, *51*, 104396. [[CrossRef](#)]
25. Liu, D.; Li, L.; Song, Y.; Wu, L.; Peng, Y. Hybrid state of charge estimation for lithium-ion battery under dynamic operating conditions. *Int. J. Electr. Power Energy Syst.* **2019**, *110*, 48–61. [[CrossRef](#)]
26. Pop, V.; Bergveld, H.; Notten, P.; Veld, J.O.H.; Regtien, P. Accuracy analysis of the State-of-Charge and remaining run-time determination for lithium-ion batteries. *Measurement* **2009**, *42*, 1131–1138. [[CrossRef](#)]
27. Wang, J.; Cao, B.; Chen, Q.; Wang, F. Combined state of charge estimator for electric vehicle battery pack. *Control Eng. Pract.* **2007**, *15*, 1569–1576. [[CrossRef](#)]
28. Kim, J.; Cho, B.H. State-of-Charge Estimation and State-of-Health Prediction of a Li-Ion Degraded Battery Based on an EKF Combined with a Per-Unit System. *IEEE Trans. Veh. Technol.* **2011**, *60*, 4249–4260. [[CrossRef](#)]
29. Abdollahzadeh, B.; Gharehchopogh, F.S.; Mirjalili, S. African vultures optimization algorithm: A new nature-inspired metaheuristic algorithm for global optimization problems. *Comput. Ind. Eng.* **2021**, *158*, 107408. [[CrossRef](#)]
30. Fahmy, H.M.; Sweif, R.A.; Hasaniien, H.M.; Tostado-Véliz, M.; Alharbi, M.; Jurado, F. Parameter Identification of Lithium-Ion Battery Model Based on African Vultures Optimization Algorithm. *Mathematics* **2023**, *11*, 2215. [[CrossRef](#)]
31. Movassagh, K.; Raihan, A.; Balasingam, B.; Pattipati, K. A Critical Look at Coulomb Counting Approach for State of Charge Estimation in Batteries. *Energies* **2021**, *14*, 4074. [[CrossRef](#)]
32. Lv, J.; Jiang, B.; Wang, X.; Liu, Y.; Fu, Y. Estimation of the State of Charge of Lithium Batteries Based on Adaptive Unscented Kalman Filter Algorithm. *Electronics* **2020**, *9*, 1425. [[CrossRef](#)]

Disclaimer/Publisher's Note: The statements, opinions and data contained in all publications are solely those of the individual author(s) and contributor(s) and not of MDPI and/or the editor(s). MDPI and/or the editor(s) disclaim responsibility for any injury to people or property resulting from any ideas, methods, instructions or products referred to in the content.